Original article

Design, synthesis and *in vitro* biological activities of coumarin linked 1,3,4-oxadiazole hybrids as potential multi-target directed anti-Alzheimer agents

Namy George, Bushra Al Sabahi, Majed AbuKhader, Khalid Al Balushi, Md. Jawaid Akhtar, Shah Alam Khan *

College of Pharmacy, National University of Science and Technology, PO Box 620, PC 130, Muscat, Oman

ABSTRACT

Introduction: Alzheimer's disease (AD) is one of the most common and prevalent forms of neurodegenerative diseases. Coumarin is a versatile scaffold that exhibits a wide range of biological properties including cholinesterase inhibitory activity and therefore is an important heterocyclic moiety to develop anti-AD drugs.
Objectives: This study aimed to design and synthesize coumarin linked 1,3,4-oxadiazole hybrid derivatives as multi-target directed ligands (MTDLs) and to investigate their *in vitro* anticholinesterase, antioxidant and anti-inflammatory activities.
Methods: Two series (**4a-n** and **7a-m**) of low molecular weight ligands (27 compounds) containing coumarin linked 1,3,4-oxadiazole hybrids were synthesized and their chemical structures were characterized using analytical data. *In vitro* acetylcholinesterase (AChE), butyrylcholinesterase (BuChE) inhibitory activity, antioxidant activity and cyclooxygenase (COX) inhibitory activity were investigated following standard spectrophotometric methods. Molecular docking studies to predict the binding mode with AChE and BuChE in addition to the pharmacokinetic profile of the synthesized compounds were studied with the help of online cheminformatics software.
Results: Amongst the tested compounds for anticholinesterase activity, **4e** and **4g** hybrid derivatives were found to be the most potent AChE inhibitors (IC$_{50}$ values = 29.56 and 28.68 μM), respectively. Compound **4m** exhibited the maximum inhibitory activity against BuChE (IC$_{50}$ value = 23.97 μM). Compounds **4g** and **4e** also showed higher selectivity index (SI) of 1.652 and 1.552 as compared to standard galantamine (SI = 1.132). Molecular docking studies revealed that **4g** and **4e,** two most potent AChE inhibitors identified through *in vitro* assay, binds well to AChE (binding energy scores of −9.7 and −10.1 Kcal/Mol). Synthesized hybrid molecules also exhibited good to excellent *in vitro* antioxidant and anti-inflammatory activities.
Conclusion: Based on the results of *in vitro* and *in-silico* studies, it could be concluded that coumarin-oxadiazole hybrids acts as MTDLs and are promising source of anti-AD drugs. Further detailed investigations and modification of these compounds can lead to the development of highly potent therapeutics for the treatment of AD.

1. Introduction

Alzheimer's disease (AD) is one of the most common and prevalent forms of neurodegenerative diseases. It is a neurodegenerative disorder of cortex that is one of the most complex, perplexing and progressive diseases that clinicians confront (Liu et al., 2019, Breijyeh and Karaman 2020, Gupta et al., 2020). Dementia is AD's main clinical symptom, that is responsible for progressive impairment of cognitive skills, memory loss accompanied with confusion and difficulty in learning and performing daily routine activities (Small and Cappai 2006). AD is considered to be the most ordinary

* Corresponding author at: Dept. of Pharmaceutical Chemistry, College of Pharmacy, National University of Science and Technology, PO Box 620, PC 130 Muscat, Oman.
E-mail address: shahalam@nu.edu.om (S.A. Khan).

root cause of elderly dementia. According to the WHO, roughly 40 million individuals across the globe were battling with AD in 2012, and this number is predicted to increase at a much faster rate, i.e., it will nearly double in next 20 years (WHO 2012). Further, it has been predicted that nearly one person out of 85 will live with AD by 2050 (Brookmeyer et al., 2007). As per the WHO estimates for the period 2000–2019; (i) morbidity and mortality due to AD and other non-communicable diseases is on rise, (ii) mortality in women (65%) was more than men, and (iii) it is among the top ten causes of death worldwide but number three killer in US and Europe in 2019. Similar to cancer, cardiovascular illness, depression, stroke and other top ten killers, AD imposes a financial burden on patients, immediate family members, and healthcare providers, according to a published analysis. (Wimo et al., 2013, Azmi et al., 2022).

Although the exact pathophysiological mechanisms underlying AD are not fully understood, recent advances have been made in understanding the underlying causes of the disease that will certainly help in developing better therapeutics. The pathogenesis of AD has been shown to involve multiple pathways such as inadequate level of acetylcholine (ACh) neurotransmitter in synaptic cleft, abnormal accumulation, aggregation and problem in clearance of extracellular beta-amyloid (Aβ) peptide, increased phosphorylation and aggregation of tau protein forming neurofibrillary tangles (NFTs) inside the nerve cell, neuroinflammation and development of oxidative stress, etc., all contribute to the progression of this senile disease (Francis et al., 1999, Cheignon et al., 2018, Breijyeh and Karaman 2020, Athar et al., 2021, Husain et al., 2021). Presence of intracellular NFTs and extracellular Aβ in amyloid plaques are considered as the pathological hallmarks of AD (Lovell et al., 2004, Guillozet-Bongaarts et al., 2005). Abnormal deposition, misfolding and inadequate clearance of these protein aggregates cause synaptic transmission dysfunction followed by nerve cell death in the brain's cortex and limbic regions (Kumar and Singh, 2015).

Over the past few decades, medicinal chemists have targeted cholinesterases viz., acetylcholinesterase (AChE) and butyrylcholinesterase (BuChE) enzymes to develop anti-AD therapy. Anticholinesterase agents' primarily selective AChE inhibitors were paid special attention for AD drug development. So far, there are only five US-FDA approved anti-Alzheimer's molecules available on the market to treat AD symptoms, including donepezil (synthetic molecule), a natural alkaloid (galantamine), memantine (NMDA antagonist), aducanumab (Aβ directed antibody), and rivastigmine based on chemical structure of natural physostigmine alkaloid. (Fig. 1). Almost all the clinically used AD drugs improve cognitive functions by acting as AChE inhibitors. However, the clinical utility of AChEIs is limited by their ability to penetrate through the blood–brain barrier (BBB) (Hamulakova et al., 2016). Other molecules in the interventional trials stage of drug development (Blume et al., 2018), more or less targets only one pathway that similar to existing therapy may provide only a short-term symptomatic relief for this complex disease with a multifaceted etiology. Also, it is evidenced that there is a decrease activity of the AChE and slight increase in the activity of BuChE. The inhibition of BuChE is desirable for the design of compounds as Anti-Alzheimer drugs but strong inhibition results in peripheral side-effects such as nausea, vomiting, and diarrhea (Shaik et al., 2016, Macklin and Schwans 2020). Considering the above facts, it seems that the ideal approach lies in identification, rational design, and development of new therapeutic modalities for the AD which can act against both these enzymes i.e., development of potent cholinesterase inhibitors (ChEIs). Oxidative stress initiates the aggregation of Aβ and tau proteins hyperphosphorylation evidenced in early pathological pathway for the development of AD (Liu et al., 2015, Cheignon et al., 2018). Anti-inflammatory drugs might also lessen the risk of AD as the people with rheumatoid arthritis has low prevalence of dementia (Martyn 2003). Thus, antioxidants and the anti-inflammatory action are additional approaches for the treatment for the AD. Recently, hybridization techniques based on multi-target directed ligands (MTDLs) have generated a lot of interest in order to develop or identify potential anti-AD agents that act on more than one pathological pathways. MTDLs are therefore considered as potential weapons in the fight against a century old neurological disease (Cavalli et al., 2008, Simone Tranches Dias and Viegas 2014, Benek et al., 2020, Makhaeva et al., 2020, Chaves et al., 2021, Husain et al., 2021).

Coumarin derivatives are extensively researched bioflavonoids for its medicinal values such as potent anti-coagulant (warfarin), anti-inflammatory, antimicrobial (antibacterial & antiviral), and
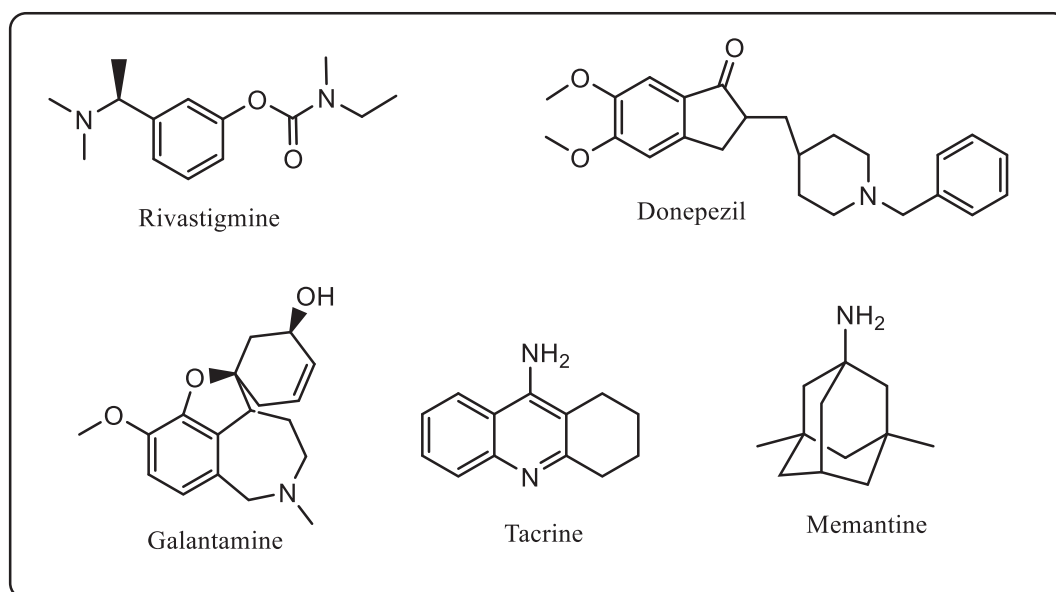

Fig. 1. Structures of clinical AChE inhibitors developed for AD.

anti-carcinogenic actions, amidst the various pharmacologically relevant targets. Recent *in-vitro* studies have proven the ability of coumarin moiety to inhibit cholinesterase enzymes. Coumarin nucleus also exhibits various inhibitory effects towards different aspects of AD such as β-secretase-1 (BACE-1) inhibition, cyclooxygenase (COX)/lipooxygenase (LOX) antagonist, cannabinoid receptor 2 (CB2) antagonist, gamma amino butyric acid (GABA) receptor agonist, *N*-methyl D aspartate (NMDA) receptor antagonist, and monoamine oxidase (MAO) inhibitor (Lee et al., 2018, Stefanachi et al., 2018, Annunziata et al., 2020, Moya-Alvarado et al., 2021). Docking studies performed with 2H-chromen-2-one highlights the binding ability of this nucleus to peripheral anionic site (PAS) of both the isoforms of cholinesterase, mimicking the natural substrate of the enzyme. Therefore, medicinal chemists developing drugs for AD have considered coumarin as a privileged scaffold for hybridization with other pharmacophores having capability to interact with other targets. Phenolic acids also demonstrate inhibitory effect on both AChE and BuChE as well as formation of β-peptide (Aβ) fibrils (Szwajgier et al., 2017). Recently one of the works carried out by Nazari *et al.,* showed oxadiazole derivatives acts as selective BuChE inhibitor (Nazari et al., 2021). Zhang *et al.,* also prepared coumarin and 1,2,4-oxadizole hybrid derivatives as a source of selective BuChE inhibitors possessing beneficial neuroprotective actions (Zhang et al., 2019). In the preliminary computational study, one prototype compound from each series (with gallic acid as phenolic acid) has been predicted to exhibit excellent enzyme inhibitory activities and was devoid of any toxicity. We therefore synthesized two libraries of novel trihybrid molecules by clubbing coumarin pharmacophoric part with polyphenolic acid and 1,3,4- oxadiazole moiety in anticipation that

the proposed compounds will be able to show antioxidant, anti-inflammatory, and anticholinesterase activities (Fig. 2). The coumarin and the oxadiazole ring connected with the methoxy linkers may allow the interaction of the coumarin and the phenolic acid end with the sites (catalytic active site (CAS) and PAS) on the enzyme AChE to inhibit its activity (Macklin and Schwans 2020). The rationale for the synthesis of target molecules is outlined in Fig. 2.

2. Materials and methods

Chemical reagents and solvents of Sigma Aldrich, SD Fine and SRL were purchased through a local supplier. All the chemicals were of high purity (analytical grade) and were used in the experiment as such. Certain analytical preparations and standard procedures are followed as reported in the literature (Azmi et al., 2020, Azmi et al., 2021). BuChE enzyme inhibitory assay Kit and COX enzyme activity assay kits were purchased from BioVision and Cayman Chemicals, respectively. Ready to use thin-layer chromatography (TLC) aluminum plates (silica gel 60 F_{254}) for monitoring the chemical reaction and for checking the purity of synthesized compounds were purchased from Merck. TLC plates were developed in a mobile phase consisting of methanol: ethyl acetate: petroleum ether (1:1:2) and were visualized in the iodine chamber. Melting points of the compounds were checked using a BioCote® melting point apparatus and are uncorrected. Infra-Red (IR) spectra were acquired on Shimadzu (FTIR-8400S) machine using KBr pellet method. A 600 MHz Bruker Ascent nuclear magnetic resonance (NMR) spectrometer was used for recording [1]H
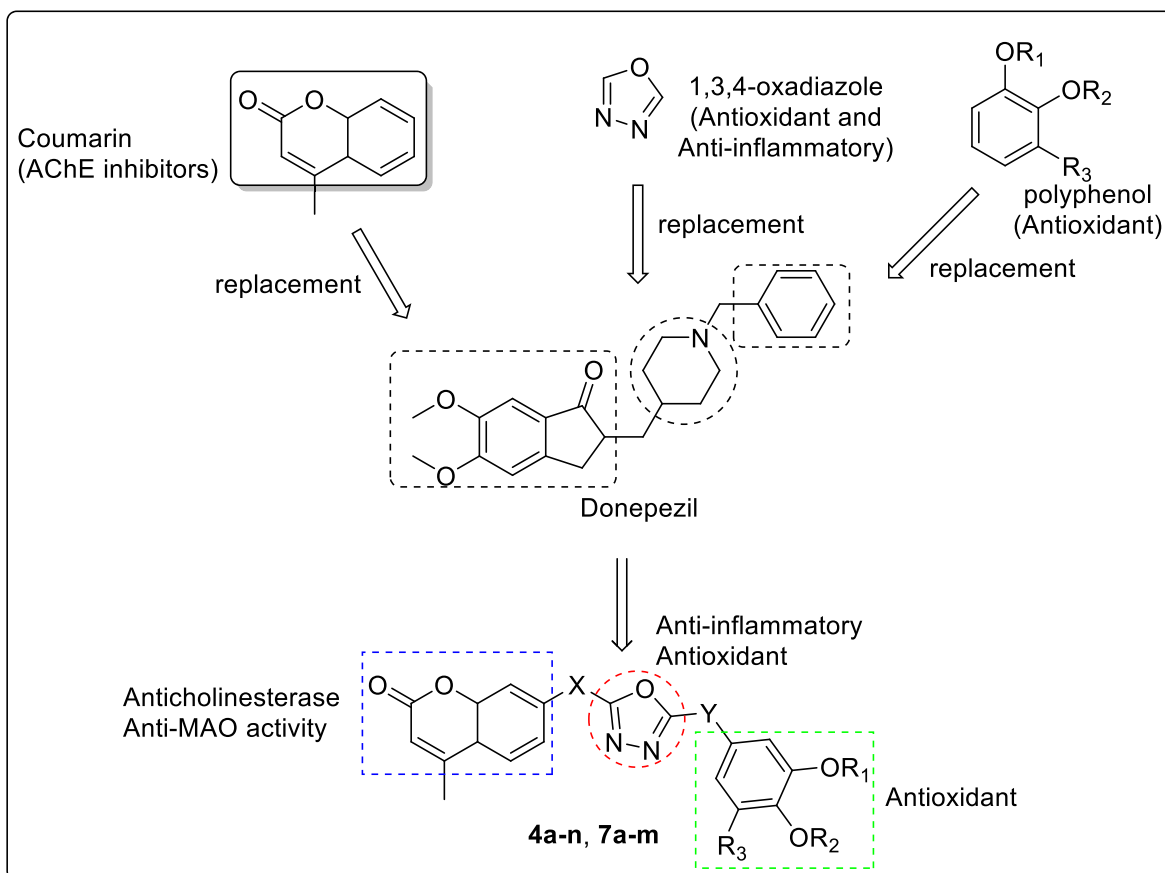

Fig. 2. Rational design protocol for the preparation of coumarin bearing 1,3,4-oxadiazole and phenolic acid hybrids as Anti-Alzheimer's agents.

NMR and ^{13}C NMR spectra in DMSO d_6 and pyridine d_5 solvents. Mass spectra were recorded using Agilent HPLC qTOF 6530 instrument using ESI mode.

2.1. Synthesis

2.1.1. Synthesis of ethyl 2-((4-methyl-2-oxo-2H-chromen-7-yl)oxy) acetate (2)

A mixture of 7-hydroxy-4-methyl coumarin (1) (5.6 mM) and ethylchloroacetate (8.5 mM) in dry dimethylformamide (DMF) (25 mL) was refluxed at 80 °C on a water bath for 10 h in the presence of potassium carbonate. After the completion of the reaction, potassium carbonate was filtered, and the mixture was poured on to the ice-cold water to obtain the precipitates of the product. The crude product was filtered and recrystallized using ethanol to obtain the TLC pure compound ethyl 2-[(4-methyl-2-oxo-2H-chromen-7-yl)oxy)acetate. m.p. 90–91 °C (Literature; 88–90 °C- (Khan and Akhtar 2003)); yield:78%.

2.1.2. Synthesis of 2-((4-methyl-2-oxo-2H-chromen-7-yl)oxy) acetohydrazide (3)

It was prepared as per the reported method. Briefly, hydrazine hydrate (15 mM) was mixed with compound 2 (10 mM) in 25 mL of absolute ethanol and the resulting mixture was gently refluxed for 4–6 h. The reaction mixture was concentrated and then cooled to obtain a solid product. Crude solid product was recrystallized in ethanol to get TLC pure compound. m.p. 201–203 °C (Literature; 198–200 °C- (Khan and Akhtar 2003)); yield: 89.9 %.

2.1.3. General procedure for the synthesis of 7-(5-substituted aryl)-1,3,4- oxadiazol-2-yl) methoxy)-4-methyl-2H-chromen-2-one (4a-n)

To a mixture of compound 3 (10 mM) and various substituted phenolic acids (10 mM), 3 mL of cyclizing agent phosphorus oxychloride (POCl$_3$) was added drop wise and then the mixture was refluxed for approximately 6 h. The progress of the chemical reaction was monitored by TLC and after confirmation of the completion of reaction, the content was cooled, poured on to crushed ice and stirred continuously to neutralize the acidic content present. Furthermore, the mixture was neutralized by adding sufficient quantity of 10% sodium bicarbonate solution until neutral pH was obtained. The resulting solution was filtered and purified by recrystallization using ethanol: DMF (1:1) to obtain pure crystalline coumarin − 1,3,4-oxadiazole hybrid derivative in good yield.

2.1.3.1. (E)-7-((5-(3-hydroxy-2-methoxystyryl)-1,3,4- oxadiazol-2-yl) methoxy)-4-methyl-2H-chromen-2-one (4a). It was synthesized by reacting 3 and ferulic acid following the general procedure described above. % Yield: 96.5; m.p. 253–255 °C; R_f: 0.62; IR (KBr, cm^{-1}); 3464.2 (phenolic O–H), 1560.4 (C = N str), 1720.5 (lactone-C = O str), 1815 (aromatic C–H str), 3100–3000 and 2914.5 (alkane C–H str); ^{1}H NMR (DMSO d_6, 600 MHz): δ 2.40 (s, 3H, CH$_3$), 3.88 (s, 3H, –OCH$_3$), 5.38 (s, 2H, CH$_2$), 6.23 (s, 1H, C-3H of coumarin), 7.22 (d, 2H, –CH = CH, J = 7.3 Hz), 7.01–7.72 (m, 6H, Ar), 9.48 (s, 1H, –OH); ^{13}C NMR (DMSO d_6, 150 MHz); δ 17.9 (CH$_3$), 61.7 (OCH$_3$), 72.4 (CH$_2$), 111–154 (Ar), 133 (=C), 160.8 (C = O), 163.2; MS (C$_{22}$H$_{18}$N$_2$O$_6$, ESI) m/z: 407.43 [M + H]$^+$.

2.1.3.2. 7-((5-(4-hydroxyphenethyl)-1,3,4-oxadiazol-2-yl)methoxy)-4-methyl-2H-chromen-2-one (4b). It was synthesized by reacting 3 and 3-(4-hydroxyphenyl) propionic acid following the general procedure described above. % Yield: 68.6; m.p. 117–120 °C; R_f: 0.50; IR (KBr, cm^{-1}); 3433.5 (phenolic OH str), 1580.5 (C = N str), 1749.5 (lactone-C = O str), 1834.3 (aromatic C–H str) and 2933.8 (alkane C–H str); ^{1}H NMR (DMSO d_6, 600 MHz): δ 2.40 (s, 3H,

CH$_3$), 2.82 (t, 2H, –CH$_2$-CH$_2$–), 3.49 (s, 3H, –CH$_2$-CH$_2$–), 5.39 (s, 2H, CH$_2$), 6.23 (s, 1H, C-3H of coumarin), 6.68–7.72 (m, 7H, Ar), 9.06 (s, 1H, –OH); ^{13}C NMR (DMSO d_6, 150 MHz): δ 19.8 (CH$_3$), 32.4, 37.1 (CH$_2$-CH$_2$), 72.3 (–OCH$_2$–), 104–160.2 (Ar), 113.6 (=C),160.8 (C = O), 161.3; MS (C$_{21}$H$_{18}$N$_2$O$_5$; ESI) m/z: 379.42 [M + H]$^+$.

2.1.3.3. 7-((5-(4-hydroxy-3-methoxyphenyl)-1,3,4-oxadiazol-2-yl) methoxy)-4-methyl-2H-chromen-2-one (4c). It was synthesized by reacting 3 and vanillic acid following the general procedure described above. % Yield: 79.2; m.p. 270–273 °C; R_f: 0.42; IR (KBr, cm^{-1}); 3450.8 (phenolic O–H str), 1562.4 (C = N str), 1737.9 (lactone-C = O str), 1803.5 (aromatic C–H str), 1687.7 (C = O str) and 3012.9 (alkane C–H str); ^{1}H NMR (DMSO d_6, 600 MHz): δ 2.47 (s, 3H, CH$_3$), 3.7 (s, 3H, –OCH$_3$), 5.4 (s, 2H,CH$_2$), 6.6 (s, 1H, C-3H of coumarin), 7.05–7.45 (m, 6H, Ar), 9.83 (s, 1H, –OH); ^{13}C NMR (DMSO d_6, 150 MHz): δ 18.7 (CH$_3$), 55.1 (OCH$_3$), 70.3 (CH$_2$), 111–160 (Ar), 160.8 (C = O), 165.2 (C of oxadiazole);); MS (C$_{20}$H$_{16}$N$_2$O$_6$; ESI) m/z: 381.39 [M + H]$^+$.

2.1.3.4. 7-((5-(3,4-dimethoxyphenyl)-1,3,4-oxadiazol-2-yl)methoxy)-4-methyl-2H-chromen-2-one (4d). It was synthesized by reacting 3 and 3,4 dimethoxybenzoic acid (veratric acid) following the general procedure described above. % Yield: 75.1; m.p. 130–132 °C; R_f: 0.45; IR (KBr, cm^{-1}); 1560.4 (C = N str), 1721 (lactone-C = O str), 1834.4 for aromatic (C–H str) and 2989.6 (alkane C–H str); ^{1}H NMR (DMSO d_6, 600 MHz): δ 2.20 (s, 3H, CH$_3$), 3.53 (s, 3H, –OCH$_3$), 3.91 (s, 3H, –OCH$_3$), 5.39 (s, 2H, –CH$_2$), 6.34 (s, 1H, C-3H of coumarin), 7.2–7.70 (m, 6H, Ar); ^{13}C NMR (DMSO d_6, 150 MHz): δ 18.2 (CH$_3$), 56.1 (2 × OCH$_3$), 72.3 (CH$_2$), 108–160 (Ar), 162.8 (C = O), 166.2; MS (C$_{21}$H$_{18}$N$_2$O$_6$; ESI) m/z: 395.41 [M + H]$^+$.

2.1.3.5. 7-((5-(3,4-dihydroxyphenyl)-1,3,4-oxadiazol-2-yl)methoxy)-4-methyl-2H-chromen-2-one (4e). It was synthesized by reacting 3 and 3,4-dihydroxybenzoic acid following the general procedure described above. % Yield: 95.1; m.p. 254–257 °C; R_f: 0.60; IR (KBr, cm^{-1}); 3423.7 (phenolic O–H str), 1560.5 (C = N str), 1739.8 (lactone-C = O str), 1830.5 (aromatic C–H str), and 2918 (alkane C–H str); ^{1}H NMR (DMSO d_6, 600 MHz): δ 2.52 (s, 3H, CH$_3$), 5.39 (s, 2H, CH$_2$), 6.33 (s, 1H, C-3H of coumarin), 6.83–7.72 (m, 6H, Ar), 9.48 (s, 2H, 2 × OH); ^{13}C NMR (DMSO d_6, 150 MHz): δ 19.1 (CH$_3$), 70.3 (CH$_2$), 112.4 (-C =), 104–160 (Ar), 160.8 (C = O), 164.4; MS (C$_{19}$H$_{14}$N$_2$O$_6$; ESI) m/z: 367.33 [M + H]$^+$.

2.1.3.6. (E)-7-((5-(3-hydroxy-2,4-dimethoxystyryl)-1,3,4-oxadiazol-2-yl)methoxy)-4-methyl-2H-chromen-2-one (4f). It was synthesized by reacting 3 and sinapic acid following the general procedure described above. % Yield: 65.4; m.p. 260–262 °C; R_f: 0.48; IR (KBr, cm^{-1}); 3425.69 (phenolic O–H str), 1560.46 (C = N str), 1737.92 (lactone-C = O str), 1872.91 (aromatic C–H str), 3103.5 (alkene C–H str); ^{1}H NMR (DMSO d_6, 600 MHz): δ 2.40 (s, 3H, CH$_3$), 3.83 & 3.89 (s, 6H, 2 × OCH$_3$), 5.39 (s, 2H,CH$_2$), 7.22 (d, 2H, CH = CH, J = 7.8 Hz), 6.23 (s, 1H, C-3H of coumarin), 6.44–7.72 (m, 5H, Ar), 8.73 (s, 1H, –OH); ^{13}C NMR (DMSO d_6, 150 MHz): δ 17.5 (CH$_3$), 56.1, 61.7 (OCH$_3$), 72.4 (CH$_2$), 104.4–154 (Ar), 124.8, 133.4 (C = C),160.8 (C = O), 163.2; MS (C$_{23}$H$_{20}$N$_2$O$_7$; ESI) m/z: 437.44 [M + H]$^+$.

2.1.3.7. 4-methyl-7-((5-(3,4,5-trihydroxyphenyl)-1,3,4-oxadiazol-2-yl)methoxy)–2H-chromen-2-one (4g). It was synthesized by reacting 3 and gallic acid following the general procedure described above. % Yield: 75.3; m.p. 250–252 °C; R_f: 0.40; IR (KBr, cm^{-1}); 3402.5 (phenolic O–H str), 1560.4 (C = N str), 1718.6 (lactone-C = O str), 1813.1 (aromatic C–H str); ^{1}H NMR (DMSO d_6, 600 MHz) δ 2.40 (s, 3H, CH$_3$), 5.39 (s, 2H, CH$_2$), 6.23 (s, 1H, C-3H

of coumarin), 6.53–7.72 (m, 6H, Ar), 8.73 (s, 1H, –OH), 9.48 (s, 2H, 2 × OH); ^{13}C NMR (DMSO d_6, 150 MHz): δ 18.4 (CH$_3$), 72.3 (CH$_2$), 104–160 (Ar), 160.8 (C = O), 162.9; MS (C$_{19}$H$_{14}$N$_2$O$_7$; ESI) m/z: 383.33 [M + H]$^+$.

2.1.3.8. (E)-7-((5-(3,4-dihydroxystyryl)-1,3,4-oxadiazol-2-yl)methoxy)-4-methyl-2H-chromen-2-one (4h). It was synthesized by reacting **3** and 3,4 dihydroxycinnamic acid (caffeic acid) following the general procedure described above. % Yield: 88.3; m.p. 254–257 °C; R$_f$: 0.53; IR (KBr, cm^{-1}); 3448 (phenolic O–H str), 1558.5 (C = N str), 1735 (lactone-C = O str), 1813.1 for aromatic (C–H str), 2914.5 (alkane C–H str), 3053 (alkene C–H str); ^{1}H NMR (DMSO d_6, 600 MHz): δ 2.40 (s, 3H, CH$_3$), 5.39 (s, 2H, CH$_2$), 6.63 (s, 1H, C-3H of coumarin), 6.99 (d, 2H, –CH = CH, J = 7.4 Hz), 6.82–7.72 (m, 6H, Ar), 9.48 (s, 1H, OH); ^{13}C NMR (DMSO d_6, 150 MHz): δ 18.1 (CH$_3$), 68.4 (CH$_2$), 111–154 (Ar), 133 (C = C), 160.8 (C = O), 164.6; MS (C$_{21}$H$_{16}$N$_2$O$_6$; ESI) m/z: 393.33 [M + H]$^+$.

2.1.3.9. (E)-7-((5-(3,4-dimethoxystyryl)-1,3,4-oxadiazol-2-yl) methoxy)-4-methyl-2H-chromen-2-one (4i). It was synthesized by reacting **3** and 3,4-dimethoxycinnamic acid following the general procedure described above. % Yield: 97.5; m.p. 154–156 °C; R$_f$: 0.43; IR (KBr, cm^{-1}); 1562.4 (C = N str), 1737.9 (lactone-C = O str), 1815 (aromatic C–H str), 2958 (alkane C–H str), 3007 (alkene C–H str), 2839 (O–CH$_3$ str); ^{1}H NMR (DMSO d_6, 600 MHz): δ 2.30 (s, 3H, CH$_3$), 3.83, 3.85 (s, 6H, 2 × OCH$_3$), 5.39 (s, 2H, CH$_2$), 6.23 (s, 1H, C-3H of coumarin), 6.99 (d, 2H, –CH = CH, J = 8.2 Hz), 7.01–7.72 (m, 6H, Ar); ^{13}C NMR (DMSO d_6, 150 MHz): δ 18.1 (CH$_3$), 53.1 (OCH$_3$), 71.1 (CH$_2$), 111–154 (Ar), 130.2, 160.8 (C = O), 163.8; MS (C$_{23}$H$_{20}$N$_2$O$_6$; ESI) m/z: 421.43 [M + H]$^+$.

2.1.3.10. (E)-7-((5-(2-(benzo[d][1,3]dioxol-5-yl)vinyl)-1,3,4-oxadiazol-2-yl)methoxy)-4-methyl-2H-chromen-2-one (4j). It was synthesized by reacting **3** and 3,4-(methylenedioxy)cinnamic acid following the general procedure described above. % Yield: 99.0; m.p. 134–136 °C; R$_f$: 0.56; IR (KBr, cm^{-1}); 1560.5 (C = N str), 1730 (lactone-C = O str), 1797.7 (aromatic C–H str), 2914.5 (alkane C–H str), 3063.1 (alkene C–H str); ^{1}H NMR (DMSO d_6, 600 MHz): δ 2.25 (s, 3H, CH$_3$), 5.39 (s, 2H, CH$_2$), 6.06 (s, 2H, -O-CH$_2$-O-), 6.23 (s, 1H, C-3H of coumarin), 6.84 (d, 2H, –CH = CH, J = 7.8 Hz), 6.94–7.72 (m, 6H, Ar); ^{13}C NMR (DMSO d_6, 150 MHz): δ 17.9 (CH$_3$), 65.4 (CH$_2$), 101.2 (CH$_2$), 108.4–154 (Ar), 160.8 (C = O), 165.1; MS (C$_{22}$H$_{16}$N$_2$O$_6$; ESI) m/z: 405.38 [M + H]$^+$.

2.1.3.11. 7-((5-(3,4-dimethoxyphenethyl)-1,3,4-oxadiazol-2-yl) methoxy)-4-methyl-2H-chromen-2-one (4k). It was synthesized by reacting **3** and 3-(3,4-dimethoxyphenyl) propionic acid following the general procedure described above. % Yield: 33.7; m.p. 222–224 °C; R$_f$: 0.40; IR (KBr, cm^{-1}); 1560.5 (C = N str), 1749 (lactone-C = O str), 1822 (aromatic C–H str), 2935 (alkane C–H str), 2897 (alkene C–H str); ^{1}H NMR (DMSO d_6, 600 MHz): δ 2.40 (s, 3H, CH$_3$), 2.82 (t, 2H, –CH$_2$-CH$_2$-), 3.49 (t, 2H, –CH$_2$), 3.75, 3.83 (s, 6H, 2 xOCH$_3$), 5.39 (s, 2H, CH$_2$), 6.23 (s, 1H, C-3H of coumarin), 6.76–7.72 (m, 6H, Ar); ^{13}C NMR (DMSO d_6, 150 MHz): δ 18.2 (CH$_3$), 32.4, 37.4 (CH$_2$), 55.1 (OCH$_3$), 72.4 (CH$_2$), 111–154 (Ar), 133.(=C), 160.8 (C = O), 164.3; MS (C$_{23}$H$_{22}$N$_2$O$_6$; ESI) m/z: 423.44 [M + H]$^+$.

2.1.3.12. 7-((5-((1E,3E)-4-(benzo[d][1,3]dioxol-5-yl)buta-1,3-dien-1-yl)-1,3,4-oxadiazol-2-yl)methoxy)-4-methyl-2H-chromen-2-one (4l). It was synthesized by reacting **3** and piperic acid following the general procedure described above. % Yield: 72.8; m.p. 138–140 °C; R$_f$: 0.52; IR (KBr, cm^{-1}); 1570.1 (C = N str), 1761.1 (lactone-C = O str), 1824.7 (aromatic C–H str), 2933.8 (alkane C–H str), 2863 (O–CH$_3$ str); ^{1}H NMR (C$_6$H$_5$N-d_5, 600 MHz): δ 2.12 (s, 3H, CH$_3$), 4.94 (s, 2H, CH$_2$), 6.06 (s, 2H, -O-CH$_2$-O-), 6.16 (s, 1H, C-3H of coumarin), 6.39 (d, 2H,

–C<u>H</u> = CH), 7.03 (m, 2H, CH = C<u>H</u>-C<u>H</u> = CH), 7.18 (d, 1H,–CH = C<u>H</u>, J = 7.4 <u>Hz</u>), 6.94–7.72 (m, 6H, Ar); ^{13}C NMR (C$_6$H$_5$N-d_5, 150 MHz): δ 17.9 (CH$_3$), 67.8 (CH$_2$), 101.8 (CH$_2$), 106.2–155.3 (Ar), 131.1 (=C), 160.7 (C = O), 169.1 (C of oxadiazole); MS (C$_{24}$H$_{18}$N$_2$O$_6$; ESI) m/z: 431.12 [M + H]$^+$.

2.1.3.13. 7-((5-(benzo[d][1,3]dioxol-4-ylmethyl)-1,3,4-oxadiazol-2-yl) methoxy)-4-methyl-2H-chromen-2-one (4m). It was synthesized by reacting **3** and 3,4-(Methylenedioxy)phenylacetic acid following the general procedure described above. % Yield: 71.9; m.p. 180–182 °C; R$_f$: 0.45; IR (KBr, cm^{-1}); 1560.5 (C = N str), 1720.6 (lactone-C = O str), 1801.6 (aromatic C–H str), 2987 (alkane C–H str), 1612 (C = O str); ^{1}H NMR (C$_6$H$_5$N-d_5, 600 MHz): δ 2.40 (s, 3H, CH$_3$), 3.81 (s, 2H, CH$_2$), 5.39 (s, 2H, –OCH$_2$), 6.07 (s, 2H, -O-CH$_2$-O-), 6.23 (s, 1H, C-3H of coumarin), 6.84–7.72 (m, 6H, Ar); ^{13}C NMR (C$_6$H$_5$N-d_5, 150 MHz): δ 18.0 (CH$_3$), 31.2 (CH$_2$), 60.5 (CH$_2$), 101.2 (O-CH$_2$-O-), 108.2–155.4 (Ar), 112.3 (=C),160.6 (C = O), 163.6; MS (C$_{21}$H$_{16}$N$_2$O$_6$; ESI) m/z: 393.10 [M + H]$^+$.

2.1.3.14. 7-((5-(benzo[d][1,3]dioxol-5-yl)-1,3,4-oxadiazol-2-yl)methoxy)-4-methyl-2H-chromen-2-one (4n). It was synthesized by reacting **3** and piperonylic acid following the general procedure described above. % Yield: 89.3; m.p. 257–259 °C; R$_f$: 0.56; IR (KBr, cm^{-1}); 1560.5 (C = N str), 1728.3 (lactone-C = O str), 1818 (aromatic C–H str), 2920.3 (alkane C–H str), 1676.2 (C = O str); ^{1}H NMR (DMSO d_6, 600 MHz): δ 2.40 (s, 3H, CH$_3$), 5.39 (s, 2H, –OCH$_2$), 6.07 (s, 2H, -O-CH$_2$-O-), 6.23 (s, 1H, C-3H of coumarin), 7.0–7.72 (m, 6H, Ar); ^{13}C NMR (DMSO d_6, 150 MHz): δ 19.4 (CH$_3$), 72.4 (CH$_2$), 101.2 (O-CH$_2$-O-), 108.4–154 (Ar), 112.3 (=C), 160.8 (C = O), 163.1; MS (C$_{20}$H$_{14}$N$_2$O$_6$; ESI) m/z: 379.32 [M + H]$^+$.

2.1.4. Synthesis of ethyl 2-oxo-2H-chromene-3-carboxylate (5)

It was synthesized by reacting a mixture of salicylaldehyde (10 mM) and diethylmalonate (10 mM) in the presence of *L*-proline (30 mg) as a catalyst following Knoevenagel Condensation reaction. The reaction -mixture was heated for 30–40 min in solvent free condition which upon cooling produced yellow solid. The obtained product was recrystallized using ethanol to get pure yellow crystalline compound.. m.p. 94–95 °C (Literature; 92 °C (Karade et al., 2007)); yield: 75.2%.

2.1.5. Synthesis of 2-oxo-2H-chromene-3-carbohydrazide (6)

It was prepared as per the reported method. Briefly, hydrazine hydrate (15 mM) was mixed with a solution of compound **5** (10 mM) in 25 mL of absolute ethanol and the resulting solution was refluxed for 4–6 h. The reaction mixture was concentrated and then cooled to obtain a solid product. It was recrystallized in ethanol to obtain TLC pure compound. m.p. 136–137 °C (Literature; 136–137 °C (Khan and Akhtar 2003); yield: 47.6 %.

2.1.6. General procedure for the preparation of 3-(5-substituted aryl)-1,3,4-oxadiazol-2-yl))–2H-chromen-2-one (7a-m)

To a mixture of compound **6** (10 mM) and various substituted phenolic acids (10 mM), 3 mL of cyclizing agent phosphorus oxychloride (POCl$_3$) was added drop wise and then the mixture was refluxed for approximately 6 h. The reaction mixture on usual work up yielded the crude solid product which was filtered and purified by recrystallization using ethanol: DMF (1:1) to obtain pure crystalline coumarin − 1,3,4-oxadiazole hybrid derivative in moderate to good yield.

2.1.6.1. (E)-3-(5-(3-hydroxy-2-methoxystyryl)-1,3,4-oxadiazol-2-yl)–2H-chromen-2-one (7a). It was synthesized by reacting **6** and ferulic acid following the general procedure described above. % Yield: 43.4; m.p. 280–283 °C; R$_f$: 0.47; IR (KBr, cm^{-1}); 3446.9 (phenolic

O–H str), 1560.5 (C = N str), 1724 (lactone-C = O str), 1815.1 (aromatic C–H str), 3009.3 (alkene C–H str) and 2914.5 (alkane C–H str); ^{1}H NMR (DMSO d_6, 600 MHz): δ 3.89 (s, 3H, OCH$_3$), 7.22 (d, 2H, CH = CH, J = 8.3 Hz), 8.05 (s, 1H, H of C-4 of coumarin), 6.99–7.86 (m, 7H, Ar), 9.48 (s, 1H, OH); ^{13}C NMR (DMSO d_6, 150 MHz); δ 61.7 (OCH$_3$), 116–151.9 (Ar), 162.9 (C = O), 158.3 (C of oxadiazole); MS (C$_{20}$H$_{14}$N$_2$O$_5$; ESI) m/z: 363.12 [M + H]$^+$.

2.1.6.2. 3-(5-(4-hydroxyphenethyl)-1,3,4-oxadiazol-2-yl)–2H-chromen-2-one (7b). It was synthesized by reacting **6** and 3-(4-hydroxyphenyl) propionic acid following the general procedure described above. % Yield: 41.2; m.p. 247–250 °C; R$_f$: 0.56; IR (KBr, cm^{-1}); 3439 (phenolic O–H str), 1562.4 (C = N str), 1751.4 (lactone-C = O str), 1828 (aromatic C–H str) and 2918.4 (alkane C–H str); ^{1}H NMR (DMSO d_6, 600 MHz): δ 2.82, (t, 2H, CH$_2$), 7.22 (d, 2H, CH = CH), 8.05 (s, 1H, H of C-4 of coumarin), 6.68–7.86 (m, 8H, Ar), 9.48 (s, 1H, OH); ^{13}C NMR (DMSO d_6, 150 MHz); δ 32.5, 37.1 (CH$_2$), 115.8–151.9 (Ar), 163.2 (C = N), 160.3, 162.9 (C = O); MS (C$_{19}$H$_{14}$N$_2$O$_4$; ESI) m/z: 335.13 [M + H]$^+$.

2.1.6.3. 3-(5-(4-hydroxy-3-methoxyphenyl)-1,3,4-oxadiazol-2-yl)–2H-chromen-2-one (7c). It was synthesized by reacting **6** and vanillic acid following the general procedure described above. % Yield: 43.4; m.p. 260–262 °C; R$_f$: 0.37; IR (KBr, cm^{-1}); 3200–3600 (phenolic O–H str), 1560.5 (C = N str), 1739.8 (lactone-C = O str), 1830.5 (aromatic C–H str), and 2918 (alkane C–H str); ^{1}H NMR (DMSO d_6, 600 MHz): δ 3.83 (s, 3H, OCH$_3$), 8.05 (s, 1H, H of C-4 of coumarin), 7.0–7.80 (m, 7H, Ar), 9.83 (s, 1H, OH); ^{13}C NMR (DMSO d_6, 150 MHz); δ 53.1 (OCH$_3$), 108.6–153.1 (Ar), 164.5 (C = N), 160.3, 164.3 (C = O); MS (C$_{18}$H$_{12}$N$_2$O$_5$; ESI) m/z: 337.22 [M + H]$^+$.

2.1.6.4. 3-(5-(3,4-dimethoxyphenyl)-1,3,4-oxadiazol-2-yl)–2H-chromen-2-one (7d). It was synthesized by reacting **6** and 3,4 dimethoxybenzoic acid (veratric acid) following the general procedure described above. % Yield: 50.1; m.p. 190–192 °C; R$_f$: 0.44; IR (KBr, cm^{-1}); 2860.6 (weak band for O-CH$_3$ str), 1560.4 (C = N str), 1751 (lactone-C = O str), 1832.4 (aromatic C–H str) and 2848 (alkane C–H str); ^{1}H NMR (DMSO d_6, 600 MHz): δ 3.73 & 3.9 (s, 3H, 2xOCH$_3$), 8.05 (s, 1H, H of C-4 of coumarin), 7.15–7.86 (m, 7H, Ar); ^{13}C NMR (DMSO d_6, 150 MHz); δ 52.1 (OCH$_3$), 108.2–153.1 (Ar), 164.5 (C = N), 157.8, 162.5 (C = O); MS (C$_{19}$H$_{14}$N$_2$O$_5$; ESI) m/z: 351.21 [M + H]$^+$.

2.1.6.5. 3-(5-(3,4-dimethoxyphenyl)-1,3,4-oxadiazol-2-yl)–2H-chromen-2-one (7e). It was synthesized by reacting **6** and 3,4-dihydroxybenzoic acid following the general procedure described above. % Yield: 87.0; m.p. 205–207 °C; R$_f$: 0.62; IR (KBr, cm^{-1}); 3443.4 (phenolic O–H str), 1564.3 (C = N str), 1749.4 (lactone-C = O str), 1815 for aromatic (C–H str); ^{1}H NMR (DMSO d_6, 600 MHz): δ 8.05 (s, 1H, H of C-4 of coumarin), 6.83–7.86 (m, 7H, Ar), 9.48 (s, 1H, OH); ^{13}C NMR (DMSO d_6, 150 MHz); δ 108.9–153.1 (Ar), 164.5 (C = N), 158.3, 162.2 (C = O); MS (C$_{17}$H$_{10}$N$_2$O$_5$; ESI) m/z: 323.10 [M + H]$^+$.

2.1.6.6. (E)-3-(5-(4-hydroxy-3,5-dimethoxystyryl)-1,3,4-oxadiazol-2-yl)–2H-chromen-2-one (7f). It was synthesized by reacting **6** and sinapic acid following the general procedure described above. % Yield: 57.1; m.p. 230–233 °C; R$_f$: 0.41; IR (KBr, cm^{-1}); 3433.4 (phenolic O–H), 1599 (C = N str), 1764.9 (lactone-C = O str), 1818.9 (aromatic C–H str), 2939.6 (alkane C–H str), 3011 (alkene C–H str); ^{1}H NMR (DMSO d_6, 600 MHz): δ 3.6 (s, 6H, 2 × OCH$_3$), 7.1 (d, 2H, CH = CH, J = 8.3 Hz), 8.05 (s, 1H, C-4H of coumarin), 6.44–7.72 (m, 6H, Ar), 8.73 (s, 1H, OH); ^{13}C NMR (DMSO d_6, 150 MHz); δ 51.1 (OCH$_3$), 104.4–153 (Ar), 124.8, 133.4 (C = C), 160.8 (C = O), 163.2; MS (C$_{21}$H$_{16}$N$_2$O$_6$; ESI) m/z: 393.15 [M + H]$^+$.

2.1.6.7. 3-(5-(2,3,4-trihydroxyphenyl)-1,3,4-oxadiazol-2-yl)–2H-chromen-2-one (7g). It was synthesized by reacting **6** and gallic acid following the general procedure described above. % Yield: 98.5; m.p. 249–250 °C; R$_f$: 0.41; IR (KBr, cm^{-1}); 3446.9 (phenolic O–H str), 1560.4 (C = N str), 1751.4 (lactone-C = O str), 1815.2 (aromatic C–H str), 2727.4 (alkane C–H str); ^{1}H NMR (DMSO d_6, 600 MHz): δ 8.05 (s, 1H, C-4H of coumarin), 6.39–7.86 (m, 6H, Ar), 8.73 (s, 1H, –OH), 9.48 (s, 1H, OH); ^{13}C NMR (DMSO d_6, 150 MHz); δ 106.1–160.3 (Ar), 122.8 (C = C), 162.8 (C = O), 163.5 (C = N of oxadiazole); MS (C$_{17}$H$_{10}$N$_2$O$_6$; ESI) m/z: 338.21 [M + H]$^+$.

2.1.6.8. (E)-3-(5-(3,4-dihydroxystyryl)-1,3,4-oxadiazol-2-yl)–2H-chromen-2-one (7h). It was synthesized by reacting **6** and 3,4 dihydroxycinnamic acid (caffeic acid) following the general procedure described above. % Yield: 62.3; m.p. 204–207 °C; R$_f$: 0.38; IR (KBr, cm^{-1}); 3454 (phenolic O–H str), 1560.5 (C = N str), 1737.9 (lactone-C = O str), 1813.1 (aromatic C–H str), 2914.5 (alkane C–H str), 3007 (alkene C–H str); ^{1}H NMR (DMSO d_6, 600 MHz): δ 6.91 (d, 2H, CH = CH, J = 7.4 Hz), 8.1 (s, 1H, H of C-4 of coumarin), 6.82–7.86 (m,7H, Ar), 9.48 (s, 1H, OH); ^{13}C NMR (DMSO d_6, 150 MHz); δ 115.2–151.9 (Ar), 124.8, 131.4 (C = C), 159.2 (C = O), 160.3 (C = N of oxadiazole); MS (C$_{19}$H$_{12}$N$_2$O$_5$; ESI) m/z: 348.11 [M + H]$^+$.

2.1.6.9. (E)-3-(5-(3,4-dimethoxystyryl)-1,3,4-oxadiazol-2-yl)–2H-chromen-2-one (7i). It was synthesized by reacting **6** and 3,4-dimethoxycinnamic acid following the general procedure described above. % Yield: 61.0; m.p. 184–186 °C; R$_f$: 0.50; IR (KBr, cm^{-1}); 1573 (C = N str), 1739.8 (lactone-C = O str), 1813 (aromatic C–H str), 3003 (alkane C–H str), 3450 (alkene C–H str); ^{1}H NMR (DMSO d_6, 600 MHz): δ 3.7 (s, 3H, 2 × OCH$_3$), 6.95 (d, 2H, CH = CH, J = 7.3 Hz), 7.16–7.86 (m, 7H, Ar), 8.05 (s, 1H, H of C-4 of coumarin); ^{13}C NMR (DMSO d_6, 150 MHz); δ 51.1 (OCH$_3$), 108.7–153.1 (Ar), 124.8,133.6 (C = C), 160.9 (C = O), 163.3 (C = N of oxadiazole); MS (C$_{21}$H$_{16}$N$_2$O$_5$; ESI) m/z: 376.31 [M + H]$^+$.

2.1.6.10. (E)-3-(5-(2-(benzo[d][1,3]dioxol-5-yl)vinyl)-1,3,4-oxadiazol-2-yl)–2H-chromen-2-one (7j). It was synthesized by reacting **6** and 3,4-(methylenedioxy)cinnamic acid following the general procedure described above. % Yield: 82.4; m.p. 192–195 °C; R$_f$: 0.52; IR (KBr, cm^{-1}); 1564.3 (C = N str), 1751.4 (lactone-C = O str), 1815.7 (aromatic C–H str), 2914.5 (alkane C–H str), 2897 (alkene C–H str); ^{1}H NMR (DMSO d_6, 600 MHz): δ 6.06 (s, 2H, -O-CH$_2$-O-), 7.02 (d, 2H, CH = CH, J = 7.3 Hz), 6.94–7.86 (m, 7H, Ar), 8.05 (s,1H, H of C-4 of coumarin); ^{13}C NMR (DMSO d_6, 150 MHz); δ 101.2 (CH$_2$), 105.9–153.1 (Ar), 124.8, 135.4 (C = C), 161.9 (C = O), 165.3 (C = N of oxadiazole); MS (C$_{20}$H$_{12}$N$_2$O$_5$; ESI) m/z: 360.23 [M + H]$^+$.

2.1.6.11. 3-(5-(3,4-dimethoxyphenethyl)-1,3,4-oxadiazol-2-yl)–2H-chromen-2-one (7k). It was synthesized by reacting **6** and 3-(3,4-dimethoxyphenyl)propionic acid following the general procedure described above. % Yield: 12.7; m.p. 208–210 °C; R$_f$: 0.50; IR (KBr, cm^{-1}); 1570.1 (C = N str), 1761.1 (lactone-C = O str), 1824.7 (aromatic C–H str), 2933.8 (alkane C–H str), 2863 (O-CH$_3$ str); ^{1}H NMR (DMSO d_6, 600 MHz): δ 2.82 (t, 2H, –CH$_2$-CH$_2$), 3.49 (t, 2H, CH$_2$), 3.75, 3.83 (s, 3H, 2 × OCH$_3$), 6.76–7.86 (m, 7H, Ar), 8.05 (s, 1H, H of C-4 of coumarin); ^{13}C NMR (DMSO d_6, 150 MHz); δ 32.4, 37.4 (CH$_2$), 56.1 (–OCH$_3$), 112.3–153.1 (Ar), 161.9 (C = O), 163.2 (C = N of oxadiazole); MS (C$_{21}$H$_{18}$N$_2$O$_5$; ESI) m/z: 378.12 [M + H]$^+$.

2.1.6.12. 3-(5-((1E,3E)-4-(benzo[d][1,3]dioxol-5-yl)buta-1,3-dien-1-yl)-1,3,4-oxadiazol-2-yl)–2H-chromen-2-one (7l). It was synthesized by reacting **6** and piperic acid following the general procedure described above. % Yield: 62.9; m.p. 217–220 °C; R$_f$: 0.60; IR (KBr, cm^{-1}); 1573.9 (C = N str), 1737.9 (lactone C = O str), 1815.1 (aromatic

C–H str), 2912.6 (alkane C–H str), 3028 (C = CH str); ^{1}H NMR (DMSO d_6, 600 MHz): δ 6.06 (s, 2H, -O-CH$_2$-O-), 6.65 (d, 2H, –C$\underline{H}$ = CH, J = 6.9 Hz), 6.71 (m, 2H, CH = C$\underline{H}$-C$\underline{H}$ = CH), 7.02 (d, 1H, –CH = C$\underline{H}$, $\underline{J = 8.1\ Hz}$), 6.94–7.86 (m, 7H, Ar), 8.05 (s, 1H, H of C-4 of coumarin); ^{13}C NMR (DMSO d_6, 150 MHz); $\underline{\delta}$ 101.2 (CH2), 105.9–153.1 (Ar), 128.8, 132.4 (C = C), 161.9 (C = O), 160.3 (C = N of oxadiazole); MS (C$_{22}$H$_{14}$N$_2$O$_5$; ESI) m/z: 387.16 [M + H]$^+$.

2.1.6.13. 3-(5-(benzo[d][1,3]dioxol-4-ylmethyl)-1,3,4-oxadiazol-2-yl)–2H-chromen-2-one (7m). It was synthesized by reacting **6** and 3,4-(Methylenedioxy)phenylacetic acid following the general procedure described above. % Yield: 73.9; m.p. 200–203 °C; R$_f$: 0.43; IR (KBr, cm^{-1}); 1570.1 (C = N str), 1751.4 (lactone C = O str), 1803.5 (aromatic C–H str), 2962 (alkane C–H str), 1622.2 (C = O str); ^{1}HNMR (DMSO d_6, 600 MHz): δ 3.81 (s, 2H, CH$_2$), 6.07 (s, 2H, -O-CH$_2$-O-), 6.84–7.86 (m, 7H, Ar), 8.05 (s, 1H, H of C-4 of coumarin); ^{13}C NMR (DMSO d_6, 150 MHz); δ 25.3 (–CH$_2$), 101.5 (CH$_2$), 112.3–153.1 (Ar), 124.8, 133.4 (C = C), 165.1 (C = O), 166.3 (C = N of oxadiazole); MS (C$_{19}$H$_{12}$N$_2$O$_5$; ESI) m/z: 349.24 [M + H]$^+$.

2.2. Biological activity

2.2.1. DPPH radical scavenging (antioxidant activity) assay of the designed hybrid ligands

In vitro antioxidant activity of the synthesized trihybridized coumarin linked 1,3,4-oxadiazole derivatives **4(a-n)** and **7(a-m)** was investigated using 1,1-diphenyl-2-picryl hydrazyl (DPPH) radical assay. Gallic acid was used as the standard antioxidant. Various concentrations (100, 50, 40, 30, 20 and 10 μM) of the synthesized derivatives (**4a-n** and **7a-m)** and positive control were used for the assay. To evaluate the antioxidant activity 25 μL of the test sample/standard was added to 96 well plate and was mixed thoroughly with 175 μL of DPPH in methanol solution (0.004% w/v). A control well was also maintained which did not contain sample to cancel out the inherent activity of solvent in the experiment. The plate was then kept aside in dark at room temperature for 30–45 min. The optical density of the test and standard solution was measured at 517 nm using 96 microplate bioanalyzer reader (Epoch, Biotek) (Lolak et al., 2020). The radical scavenging activity was calculated using the standard formula.

IC$_{50}$ of the designed ligands was calculated using non-linear regression analysis of the % inhibition and concentration (μM). The antioxidant property of the designed ligands was compared with the antioxidant capability of gallic acid. All the tests were carried out in triplicate and the results are reported as mean ± standard deviation (SD).

2.2.2. Evaluation of AChE inhibitory activity

A colorimetric assay was employed to evaluate AChE inhibitory activity of the designed ligands. β-naphthyl acetate (NA) was employed as the substrate for the enzyme AChE while fast blue-B salt (FB) was used as the diazonium dye forming reagent. β-NA is hydrolyzed by the enzyme AChE into naphthol and acetate. The formed naphthol then reacts with the fast blue B to form diazonium dye that gives a stable purple color. For the quantitative estimation of the dye formed, absorbance of the color intensity was measured after the reaction using a bio analyzer. For the spectrometric analysis each compound prepared in different concentrations (100, 50, 40, 30, 20, 10 μM) and 50 μL of it was added in triplicate in different wells. 50 μL of NA (0.25 mg/mL in methanol) and 50 μL of AChE were added to each well and mixed thoroughly. The microplate was then incubated at room temperature for 40 min. After 40 min, 10 μL of FB salt (0.25 mg/mL) solution in water was added to the incubated mixture and mixed well with the pipette. The absorbance of the mixture was determined at

600 nm. Blank wells containing no samples were also used to nullify the effect of solvents in the mixture. Standard drug galantamine, an AChE inhibitor, was used to compare the results (Khokar et al., 2021).

2.2.3. Evaluation of BuChE inhibitory activity

BuChE inhibitory Kit (Catalog#K516-100) was purchased from BioVision. The inhibitory assay was performed according to the method described in the product information leaflet. Briefly, 20 μL of desired concentrations of the samples were added to each well in triplicate. The enzyme BuChE was diluted 50 folds. 8 μL of the enzyme was added to each well and mixed thoroughly. The volume was adjusted to 95 μL with the assay buffer. Control well was also prepared in the same way but without adding a sample. 5 μL of DTNB solution prepared was also added to the reaction mixture. The total volume in each well was made up to 100 μL.100 μL of 120-fold diluted BuChE substrate was then added and mixed well. The plate was then kept for incubation in the dark for 20–30 min. The absorbance was measured at 412 nm and % BuChE inhibitory activity was calculated (Lolak et al., 2020).

2.2.4. Evaluation of COX inhibitory activity of the synthesized hybrids

COX activity assay kit (item no.760151) was purchased from Cayman Chemicals. The assay was performed according to the procedure outlined in the product information leaflet. Briefly, 110 μL of assay buffer, 10 μL of hemin, 10 μL of COX enzyme and 40 μL of sample were added to the sample wells in triplicate. After Incubation for 5 min, the contents were mixed uniformly in each well followed by addition of 20 μL of colorimetric substrate to each well. To initiate the reaction, 20 μL of arachidonic acid solution was added to the wells. The plates were shaken carefully and the incubated for 5 min at 25 °C.

The control well was prepared in the same manner by omitting the sample compounds. The absorbance of the mixture was recorded at 590 nm using a microplate reader and % COX inhibition was calculated (Dey et al., 2003).

2.3. In silico prediction of molecular properties, toxicity and pharmacokinetic profile

SMILES (simplified molecular-input line-entry system) notation of the prepared compounds were generated with the help of ChemSketch software. The SMILES of each compound was entered in to the Molinspiration online cheminformatic software (https://www.molinspiration.com/img/molinspiration-logo2-animated.gif) to predict their physicochemical properties (miLogP, TPSA, molecular weight, hydrogen bond acceptor, hydrogen bond donor and number of rotatable bonds). The results are presented in supplementary material. Toxicity and pharmacokinetic profile of hybrid compounds were predicted with the help of online servers namely OSIRIS and admetSAR prediction tools. The results of toxicity and pharmacokinetic profile are presented in supplementary material.

2.4. Molecular docking studies

An online docking software (https://www.mcule.com) platform was used to study the ligand-receptor interactions. The 3D structure of the enzyme AChE (PDB ID: 2CMF) and BuChE (PDB ID: 4BDS) were retrieved from Protein Data Bank (PDB). Both water molecules and bound ligands were removed from the crystal structures by using Discovery Studio Visualizer 2021 Client. Then, the crystal structure of protein was uploaded as PDB file onto the online server. The proteins selected were prepared for docking by adding polar hydrogen atoms and Gasteiger charges. We have used a binding site having coordinates of (X: 7.587061, Y: 64.755204 and Z: 58.317755) for 2CMF protein and X: 138.804639, Y:

123.637895 and Z: 38.657348 for 4BDS. The energy minimized 3D structure of ligands were uploaded in the next step.

### 2.4.1. Visualization of docking poses and docking analysis

Molecular docking studies were performed with mcule.com webserver which generated top five hits. The poses were analyzed for interaction. The best minimal binding energy pose for ligand–protein interaction was saved as a PDB file to further study docking conformation and types of bonding interaction. The downloaded poses were visualized for the ligand-target interaction using Discovery studio Visualizer. The 2D image was used to study the

amino acids residues of the active site of the receptor interacting with the designed ligands.

3. Results and discussion

3.1. Chemistry

Two libraries of coumarin linked 1,3,4-oxadiazole hybrid compounds were prepared in a single step by reacting **3** or **6** with substituted phenolic acids in presence of few mL of phosphorus oxychloride (Scheme 1a,b). Dehydrative cyclization resulted in

Scheme-1a

Scheme-1b
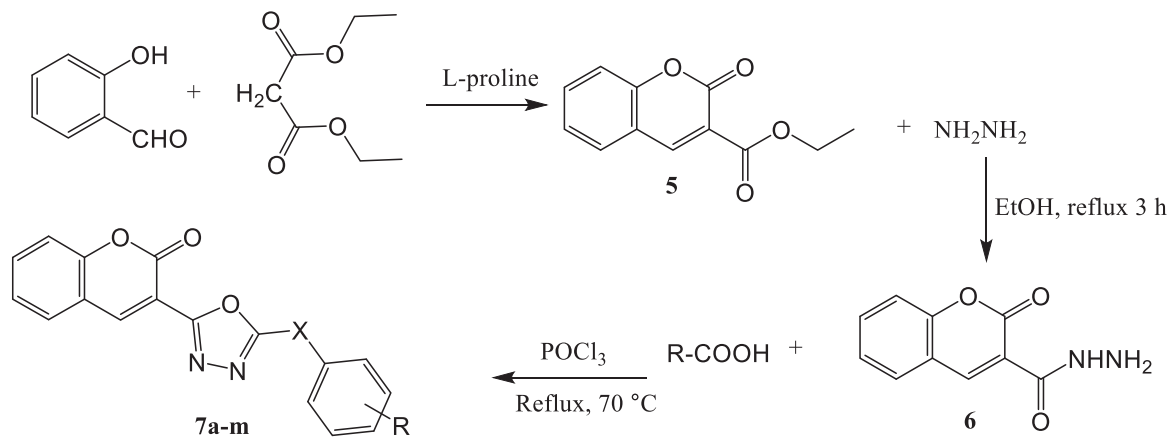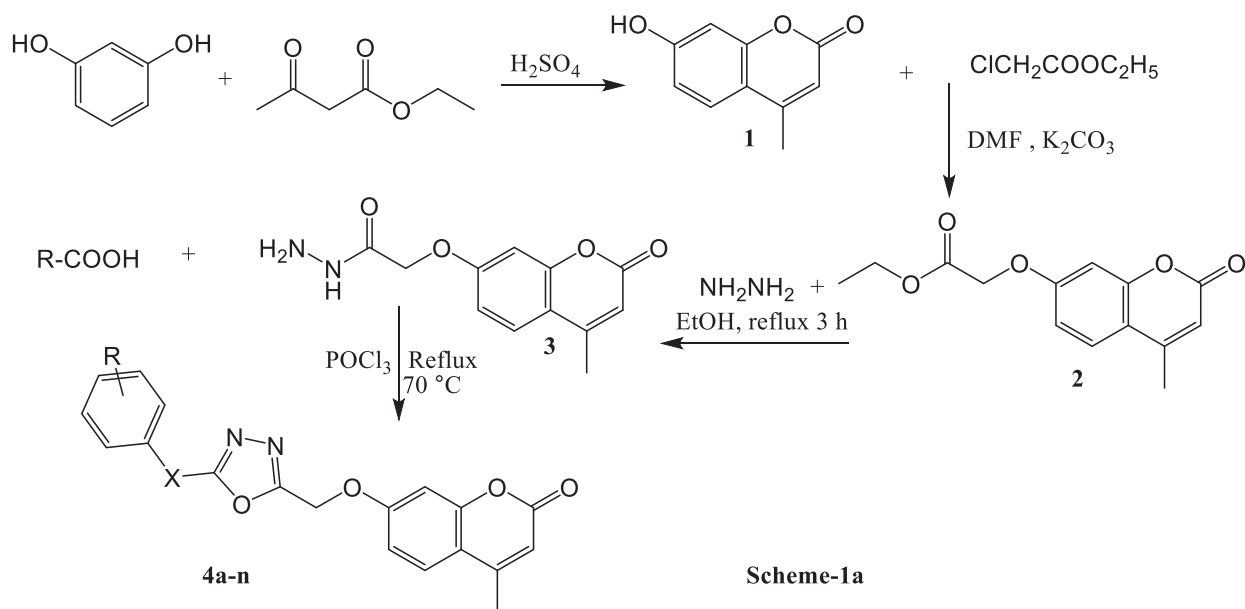
Comp.	X	R	Comp.	X	R
4a,7a	-CH=CH-	2-OCH$_3$, 3-OH	4h, 7h	-CH=CH-	3,4-OH
4b, 7b	-(CH$_2$)$_2$-	4-OH	4i, 7i	-CH=CH-	3,4-OCH$_3$
4c, 7c	--	3-OCH$_3$, 4-OH	4j, 7j	-CH=CH-	-O-CH$_2$-O-
4d,7d	--	3,4-OCH$_3$	4k, 7k	-(CH$_2$)$_2$-	3,4-OCH$_3$
4e,7e	--	3,4-OH	4l, 7l	-(CH=CH)$_2$-	-O-CH$_2$-O-
4f, 7f	-CH=CH-	3,5-OCH$_3$, 4-OH	4m, 7m	-CH$_2$-	-O-CH$_2$-O-
4g, 7g	--	3,4,5-OH	4n	----	-O-CH$_2$-O-

Scheme 1. a & b: Scheme for the synthesis of hybrid compounds.

Table 1
Results of *in vitro* anticholinesterase and antioxidant assays.

Comp.	X	R	IC$_{50}$ ± SD values (μM)			
			AChE	BuChE	DPPH	SI*
4a	−CH = CH−	2-OCH$_3$, 3-OH	51.39 ± 0.97	36.95 ± 2.91	68.39 ± 1.25	0.719
4b	-(CH$_2$)$_2$-	4-OH	64.25 ± 2.02	36.60 ± 0.71	58.08 ± 1.44	0.569
4c	−	3-OCH$_3$, 4-OH	58.34 ± 6.41	35.02 ± 0.57	69.17 ± 1.69	0.600
4d	−	3,4-OCH$_3$	159.74 ± 1.94	53.57 ± 1.21	>200	0.335
4e	−	3,4-OH	29.56 ± 3.95	45.87 ± 1.43	67.07 ± 3.46	1.552
4f	−CH = CH−	3,5-OCH$_3$, 4-OH	85.98 ± 2.59	105.93 ± 13.81	>200	1.232
4g	−	3,4,5-OH	28.68 ± 2.91	47.39 ± 2.87	65.57 ± 5.62	1.652
4h	−CH = CH−	3,4-OH	72.90 ± 2.32	38.37 ± 0.85	66.22 ± 2.95	0.526
4i	−CH = CH−	3,4-OCH$_3$	40.84 ± 1.29	85.47 ± 5.04	85.03 ± 0.61	2.092
4j	−CH = CH−	-O-CH$_2$-O-	48.69 ± 3.60	38.72 ± 2.76	81.56 ± 2.07	0.795
4k	-(CH$_2$)$_2$-	3,4-OCH$_3$	76.07 ± 4.00	81.51 ± 2.07	100.00 ± 2.14	1.124
4l	-(CH = CH)$_2$-	-O-CH$_2$-O-	48.90 ± 3.17	39.09 ± 0.90	75.18 ± 2.92	0.799
4m	−CH$_2$-	-O-CH$_2$-O-	42.06 ± 2.11	23.97 ± 5.61	75.18 ± 2.97	0.570
4n	−	-O-CH$_2$-O-	40.62 ± 3.20	65.35 ± 2.76	72.22 ± 1.46	1.609
7a	−CH = CH−	2-OCH$_3$, 3-OH	82.10 ± 4.01	34.29 ± 0.68	52.80 ± 2.50	0.418
7b	-(CH$_2$)$_2$-	4-OH	Discontinued due to solubility issues			
7c	−	3-OCH$_3$, 4-OH	42.84 ± 3.68	38.34 ± 3.42	106.16 ± 1.34	0.592
7d	−	3,4-OCH$_3$	92.25 ± 7.07	51.92 ± 3.45	66.30 ± 2.29	0.563
7e	−	3,4-OH	49.65 ± 2.98	37.76 ± 0.60	>200	0.760
7f	−CH = CH−	3,5-OCH$_3$, 4-OH	64.35 ± 3.05	34.77 ± 1.11	79.11 ± 1.25	0.540
7g	−	3,4,5-OH	43.29 ± 3.44	45.7 ± 2.02	48.12 ± 1.67	1.056
7h	−CH = CH−	3,4-OH	64.77 ± 7.77	37.07 ± 0.75	48.3 ± 1.48	0.572
7i	−CH = CH−	3,4-OCH$_3$	96.97 ± 3.39	99.2 ± 7.17	52.23 ± 1.73	1.022
7j	−CH = CH−	-O-CH$_2$-O-	50.215 ± 2.31	37.25 ± 3.77	86.81 ± 2.91	0.741
7k	-(CH$_2$)$_2$-	3,4-OCH$_3$	54.96 ± 0.98	38.43 ± 0.93	53.13 ± 2.92	0.699
7l	-(CH = CH)$_2$-	-O-CH$_2$-O-	40.64 ± 1.91	35.24 ± 1.37	90.25 ± 4.53	0.867
7m	−CH$_2$-	-O-CH$_2$-O-	43.17 ± 07	34.53 ± 1.83	113.89 ± 0.56	0.800
Galantamine	−	−	74.73 ± 5.88	84.65 ± 5.88	−	1.132
Gallic acid	−	−	−	−	65.10 ± 5.40	−

*SI = BuChE/AChE.

the formation of trihybridized coumarin tethered 1,3,4-oxadiazole derivatives (**4a-n** and **7a-m**) in good yield. Compound **3** was prepared following three steps chemical reactions. In the initial step resorcinol and ethyl acetoacetate were reacted in the presence of sulfuric acid (98%) in ice cold condition to obtain 7-hydroxy-4-methyl coumarin (**1**) which was then converted into ethyl 2-((4-methyl-2-oxo-2H-chromen-7-yl)oxy)acetate (**2**) by refluxing it with ethylchloroacetate in dry DMF in the presence of potassium carbonate at 80 °C for 10 h. Compound (**2**) on reaction with hydrazine hydrate in absolute ethanol yielded compound **3** (Scheme 1**a**). Similarly, compound **6** was synthesized in two steps. First, ethyl 2-oxo-2H-chromene-3-carboxylate (**5**) was obtained by reacting salicylaldehyde and diethylmalonate using *L*-proline as a catalyst. It was then converted to corresponding carbohydrazide by treating with hydrazine hydrate (Scheme 1**b**). The purity of the compounds was checked by TLC using ethyl acetate: methanol: petroleum ether (1:1:2) as solvent system. Compounds showed a single spot-on TLC and were found to be pure. The structures of all coumarin hybrids were characterized with the help of IR, ^{1}H & ^{13}C NMR and Mass spectral studies. The spectral data are consistent with their chemical structures. In the IR spectra lactone carbonyl absorption band appears between 1718 and 1764 cm^{-1}. The proton NMR showed characteristics peak of methoxy at 3.8 ppm, vinyl proton as 6.82 to 7.22 ppm and phenolic −OH at 8.73–9.83 ppm.

3.2. Anticholinesterase activity

AChE and BuChE inhibitory activities of the synthesized hybrid molecules (**4a-n** and **7a-m**) were evaluated by NA-FB colorimetric assay and as per modified Ellman's method respectively. The inhibitory activity of each compound was tested at five different concentrations against AChE and BuChE. The IC$_{50}$ value and the selectivity index of the compounds taking galantamine as standard are shown in Table 1. The synthesized hybrids exhibited moderate

to good inhibitory activity against both AChE and BuChE with an IC$_{50}$ in micromolar range. The results clearly showed that the presence of linker between phenolic and 1,3,4-oxadiazole have some influence on inhibition of AChE. Against AChE enzyme, series **1a** compounds (**4a-n**) showed IC$_{50}$ value from 28.68 to 159.74 μM while it was in the range of 40.64–96.97 μM for the series **1b** compounds (**7a-m**). Almost all the compounds showed better AChE inhibitory activity than the positive control galantamine (IC$_{50}$ = 74.73 ± 5.88 μM). The compounds 4-methyl-7-((5-(3,4,5-trihydroxyphenyl)-1,3,4-oxadiazol-2-yl)methoxy)–2H-chromen-2-one (**4g**) and 7-((5-(3,4-dihydroxyphenyl)-1,3,4-oxadiazol-2-yl)methoxy)-4-methyl-2H-chromen-2-one (**4e**) were noted as the two most promising AChE inhibitors which showed IC$_{50}$ values of 28.68 ± 2.91 μM and 29.56 ± 3.95 μM. It was interesting to note that among all the coumarin-oxadiazole hybrids in series **1a** where 1,3,4 oxadiazole ring is connected to 7th position of coumarin ring through –OCH$_2$ linker, compound (**4g**) with three hydroxy substituted phenyl ring at 3,4,5 position and attached directly to the 5th position of oxadiazole ring showed the best AChE inhibitory activity. Decreasing the hydroxy groups on the phenyl ring from 3,4,5 trihydroxy to 3,4 dihydroxy as in compound **4e** led to slight decrease in activity. Surprisingly, replacing either both or one of the two hydroxy groups with another electron donating functionality such as –OCH$_3$ or methylenedioxy groups in the phenyl ring connected to oxadiazole moiety without a linker decreased the activity>5-fold (**4d;** 159.74 μM) and 1.5–2-fold (**4c;** 58.34 μM; **4n**: 40.62 μM), respectively. The inhibitory activity of dihydroxy compound **4h** with the vinyl linker (CH = CH) dramatically decreased (IC$_{50}$ = 72.90 μM). The vinyl linker with the dimethoxy substitution **4i** (IC$_{50}$ = 40.84) or methylenedioxy **4j** (IC$_{50}$ 48.69 μM) and **4l** (IC$_{50}$ = 48.90 μM) showed strong inhibition as compared to compound without vinyl linker **4d (**IC$_{50}$ = 159.74 μM). Thus, vinyl linker has some influence on the level of inhibitions when the phenyl ring is substituted with dimethoxy group. Derivatives **4a** (IC$_{50}$ = 51.39

μM) and **4c** (IC$_{50}$ = 58.34 μM) with one hydroxy and methoxy group in the phenyl ring has similar inhibition and has no such influence of the vinyl group on activity. Similarly, the methylenedioxy substituted derivatives also has no effects of linkers on the levels of AChE inhibition (**4m** with methylene linker IC$_{50}$ = 42.06 μM) and **4n** without the linker (IC$_{50}$ = 40.62 μM).

The derivatives also showed similar trends of BuChE inhibition (IC$_{50}$ = 23.97–105.93 μM). It is evident from the results that when trihydroxy (**4g**; IC$_{50}$ = 47.39 μM) is replaced with dihydroxy (**4e**; IC$_{50}$ = 45.87 μM) there is slight decrease in the BuChE inhibitory activity. The most potent among the series is 7-((5-(benzo[d][1,3]dioxol-4-ylmethyl)-1,3,4-oxadiazol-2-yl)methoxy)-4-methyl-2H-chromen-2-one (**4m**) with methylene spacer and the methylenedioxy attached to the phenyl (IC$_{50}$ = 23.97 μM). The dihydroxy (IC$_{50}$; **4h** = 38.37 μM) or one methoxy and hydroxy substitution (IC$_{50}$; **4a** = 36.95 μM), (IC$_{50}$; **4c** = 35.02 μM) has no effect against the BuChE inhibitory activity having vinyl spacer. The derivatives with two methoxy groups (**4f**, **4d**, **4i**, **4k**) dramatically decreases the BuChE activity.

Compounds in the series **1b** where 1,3,4 oxadiazole ring is directly attached to the third position on coumarin, number and position of substituents on phenyl ring also seem to affect their AChE inhibitory potential. Unlike the most active trihydroxy and dihydroxy substituted compounds **4g** and **4e** of the series **1a**, their counterparts in series **1b** (compounds **7g** and **7e**) were observed to be comparatively weaker AChE inhibitors (IC$_{50}$ = 43.29 & 49.65 μM). However, compounds **7c**, **7d**, **7f**, **7h**, **7k** and **7l** were found to be more powerful than their counterparts (**4c**, **4d**, **4f**, **4h**, **4k** and **4l**) in the series **1a** (Table 1). Overall decrease in the AChE inhibitory activity of hybrid compounds observed in the presence of OCH$_3$ group in the *ortho* and *meta* positions might be due to the stearic hindrance between the similar groups.,

Series **1b** compounds also inhibited BuChE in micromolar concentration (IC$_{50}$ = 34.29–99.2 μM). Hybrid compounds in the series **1b** with no linker (methoxy linker) between the coumarin and the oxadiazole ring are selective inhibitors of BuChE (selectivity index for AChE over BuChE = <1) except **7g** and **7i** which inhibited both AChE and BuChE equally (SI = ~1). The two most potent AChE inhibitors (**4g** and **4e**) inhibited BuChE moderately (IC$_{50}$ = 47.39 and 45.87 μM) and were also found to be approximately 1.6 times more selective inhibitors towards AChE over BuChE. Structure activity relationship indicated that compounds with a methylene dioxy functionality attached to the phenyl ring (**4m**, **4l**, **4j**, **7j**, **7l** and **7m**) exhibited similar BuChE inhibitory activity (Table 1). Zhang et al., in 2019 prepared the coumarin linked 1,2,4-oxadiazole hybrids. The most potent AChEI of the series was approximately three times more potent than **4g** and **4e**. This difference in activity could be attributed to position of nitrogen atoms in the oxadiazole ring and to the presence of additional pyrrolidinyl ring in the hybrid molecules (Zhang et al., 2019).

3.3. Antioxidant activity

In vitro free radical scavenging potential of the hybrids compounds was evaluated by DPPH free radical assay method. This colorimetric method measures the reduction in the color intensity at 517 nm. DPPH produces a violet color in methanol solution but after accepting electrons from the antioxidants, it fades to yellow/pale yellow color (Molyneux 2004). The results of antioxidant activity presented in Table 1 indicate that few of the synthesized compounds **4b**, **7a**, **7g**, **7h**, **7i** and **7k** (IC$_{50}$ = 58.08, 52.80, 48.12, 48.3, 52.23 and 53.13 μM, respectively) exhibited better antioxidant activity than the reference compound gallic acid (IC$_{50}$ = 65.10 ± 5.50 μM). The two most potent AChE inhibitors viz., **4g** and **4e** displayed similar free radical scavenging potentials (IC$_{50}$ = 65.57 and 67.07 μM) at par with the standard. Compounds (**7g** and **7 h**) were identified as the most promising antioxidant agents (IC$_{50}$ = 48.12 and 48.3 μM, respectively) which contains three and two hydroxyl groups on the phenyl ring respectively.
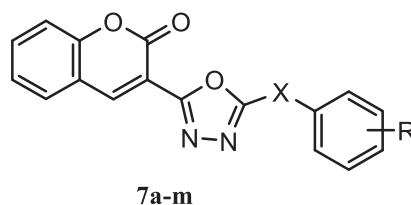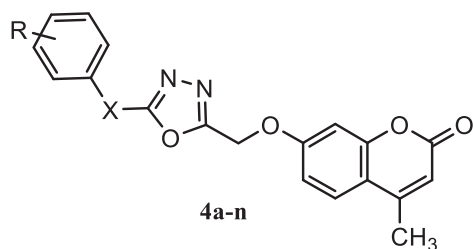
3.4. COX inhibitory activity

Nine compounds (**4e**, **4g**, **4h**, **4l**, **7a**, **7d**, **7g**, **7h** and **7k**) that exhibited potent antioxidant activity and good cholinesterase inhibition were selected for further COX inhibitory study. The activity was evaluated at 10 μM concentration and the results are illustrated in Fig. 3. Compound **7g** showed the best inhibition (72.67%) followed by **4g** (71.34%) and **4h** (70.72%). Other compounds also inhibited COX enzyme in the range of 55–72-69.74%. Results of *in vitro* biological assays provided experimental evidence that these compounds possess anti-inflammatory, antioxidant and anticholinesterase activity and therefore can act as multi-target directed ligands in the pathogenesis of AD.

3.5. In silico studies

3.5.1. Molecular docking studies

Molecular docking studies were carried out to study the AChE/BuChE- ligand interactions and to validate the results of *in vitro* experimental studies. Binding energy scores of the best pose of synthesized ligands with both the target receptors (2CMF and 4BDS) are presented in the Supplementary Table 1. Series **1a** compounds showed better binding energy scores (-7.3 to 12.0 Kcal/Mol) than series **1b** compounds (-1.3 to −9.5 Kcal/Mol) on to the AChE enzyme. Compounds **4g** and **4e** which showed the best *in vitro* AChE inhibitory activity showed binding energy scores of −9.7 and −10.1 Kcal/Mol. Compound **4e** contains 3,4-dihydroxy phenyl ring structural fragment which comes from the 3,4 dihydroxy benzoic acid while **4g** was prepared using gallic acid and therefore bears 3,4,5 trihydroxyphenyl attached at the 5th position of oxadiazole ring in the hybrid molecule. Both the
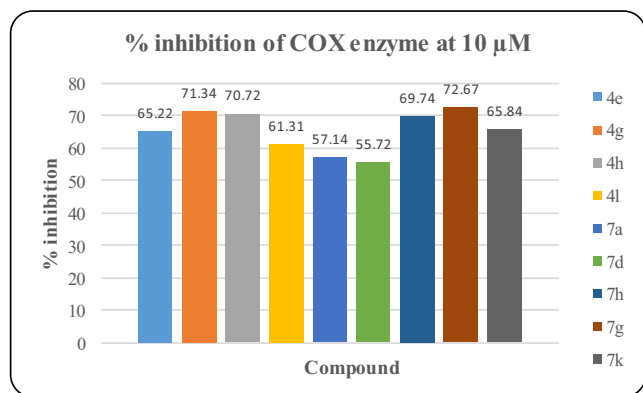

4a-n

7a-m

Fig. 3. % COX inhibitory activity of synthesized compounds at 10 μM.

molecules are from series **1a** and in contrast to series **1b** compounds consists of a 4-methyl group on the coumarin ring and an additional –O-CH$_2$- as a connecting linker between the coumarin and oxadiazole pharmacophores. Docking results of **4e** shows that the oxygen atom of the oxadiazole moiety interacts with the TYR121 present in the active site of the AChE receptor (2CMF). Apart from hydrogen bond interaction, π-π stacking (TRP84, PHE330, PHE331), van der Waals interaction and π-alkyl (TYR334) interactions were also observed (Fig. 4). It exhibited a docking score of −10.1 kcal/mol. The compound could inhibit 50% of the AChE enzyme at 29.56 μM ± 3.95. Compound **7e** which is a corresponding compound in the series **1b** with the identical 3,4-dihdroxy phenyl substituent showed a much lower docking score of −7.1 kcal/mol even though it can form two hydrogen bonds with the enzyme amino acid residues. The hydroxy group on the *meta* position on the phenyl ring and nitrogen atom in the 1,3,4-oxadiazole moiety formed hydrogen bond with the SER200 amino acid residue on the active site of the receptor. However, compound **7e** upon *in vitro* AChE inhibitory assay showed an IC$_{50}$ value of 49.65 μM ± 2.98 which is much higher than its corresponding compound in series **1b**. Also, this compound is less selective for AChE (SI = 0.76) over BuChE in comparison to **4e** (SI = 1.55). Furthermore,

4e upon docking on to the BuChE formed three hydrogen bonds, two through carbonyl oxygen (SER198 & ALA199) and one through hydroxyl group (TYR128) and showed a binding energy score of −9.6 kcal/mol. It also showed other interactions with amino acid residues including π-π (PHE329), π-alkyl (VAL288, LEU286), π-sigma (TRP231) and van der Walls interactions (Fig. 4). Thus, based on these results it can be proposed that a linker connecting the two pharmacophores (oxadiazole with coumarin) and presence of a methyl group in the coumarin moiety might help in increasing the selectivity and potency of the trihybridized molecule towards AChE. In compound **4g**, oxygen atom of the 1,3,4-oxadiazole moiety forms one hydrogen bond with the TYR121 and another hydrogen bond between *m*-OH group and PHE288 amino acid residue in the active site of the AChE receptor (Fig. 4). It showed an IC$_{50}$ value of 28.68 ± 2.91 μM for AChE inhibition and was found to be 1.65 times more selective towards AChE over BuChE with the binding energy score of −9.7 kcal/mol. The corresponding compound (**7g**) with similar structural fragment in series **1b** exhibited an IC$_{50}$ of 43.29 ± 3.44 μM against AChE and a lower docking binding score of −6.5 kcal/mol. Interactions of **7g** with the BuChE enzyme shows that it forms three hydrogen bonds with the receptor amino acid residues and has a docking score of −8.1 kcal/mol. The *p*- hydroxyl group on the phenyl ring forms a hydrogen bond with LEU286 and *m*-hydroxy group forms a hydrogen bond with TRP231. Increase in the number of hydrogen bond did not increase the interaction with the receptor which might be because hydrogen bond should be placed in favorable distance and favorable orientation for the formation of strong interaction with the receptor. On the other hand, the most promising **4g** also forms three hydrogen bonds (HIS438, SER198, ALA199) along with π-π (PHE329, TRP82), π-alkyl (VAL288, LEU286), π-sigma (TRP231) and van der Walls interactions with amino acid residues on the BuChE receptor and showed much improved binding energy score of −10.0 kcal/mol in comparison to **7g** (Fig. 4).

3.5.2. Prediction of molecular properties, toxicity and pharmacokinetic profile

Molecular properties predicted with the help of molinspiration indicated that all the synthesized hybrid compounds obey's
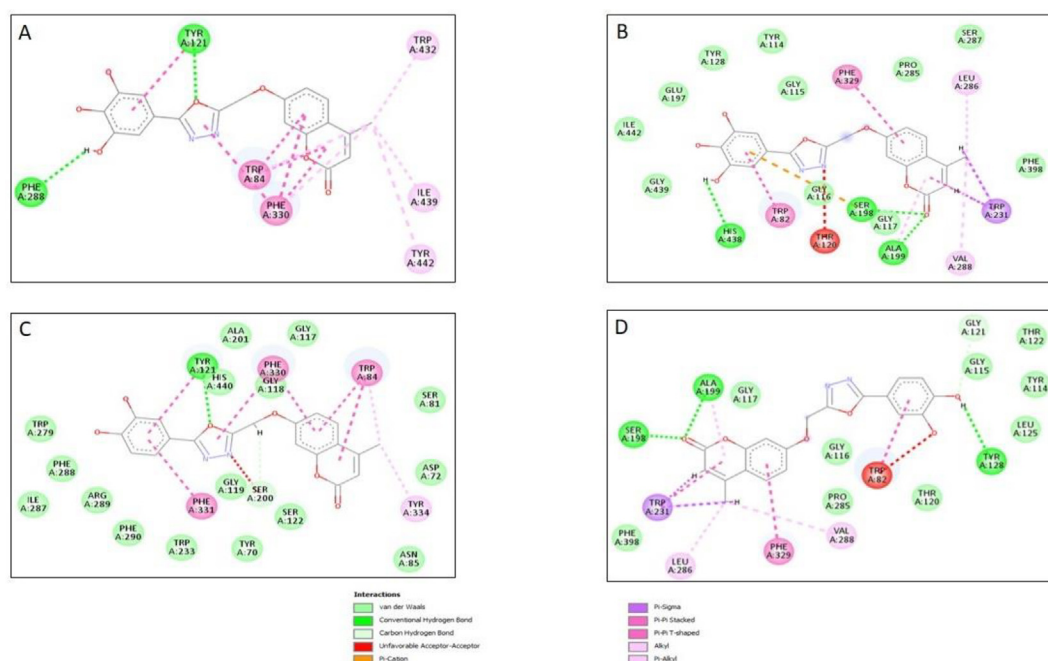

Fig. 4. 2D image of active site amino acid residue interacting with compound (A) **4g** with AChE receptor; (B) **4g** with BuChE receptor; (C) **4e** with AChE receptor and (D) **4e** with BuChE receptor.

Lipinski's rule of five and are expected to be orally bioavailable. Bioactivities predicted with the help of PASS cheminformatic online software revealed that almost all the compounds possess MAO inhibitory, antioxidant and anti-inflammatory activities. However, compounds **7j**, **7m** and **7l** were noted to be devoid of anti-inflammatory activity. OSIRIS online software predicted series **1b** compounds to be non-toxic (non-mutagenic, non-tumorigenic, non-irritant on skin with no reproductive toxic effect). However, series **1a** compounds could produce reproductive toxicity. Admet-SAR predicted high gastrointestinal absorption and moderate to good BBB permeability. All the compounds are predicted to be safer in rat acute toxicity, AMES toxicity, fish toxicity, honeybee toxicity and acute oral toxicity. Molecular properties, biological activity by PASS, OSIRIS toxicity and pharmacokinetic properties data of synthesized compounds are presented in the supplementary information.

4. Conclusion

The key intermediates of the hybrid compounds were synthesized by a Pechman reaction and the chemical structures were characterized by spectral analysis. *In-silico* prediction of biological properties by PASS revealed the coumarin-oxadiazole hybrid compounds to act on multiple targets in the pathogenesis of AD such as inhibition of cholinesterase, scavenging free radicals, decreasing oxidative stress and by reducing inflammation. *In vitro* biological assays carried out for the designed ligands showed that many of the compounds are potent inhibitors of AChE and BuChE as compared to the standard compound. The compounds **4g** and **4e** showed the most potent inhibitory activity against AChE with an IC_{50} value of 28.68 and 29.56 μM while compound **4m** showed higher activity against BuChE with IC_{50} value of 23.97 μM. The compounds **4g** and **4e** also showed higher selectivity index (SI) of 1.652 and 1.552 as compared to standard galantamine (SI = 1.132). The results showed that the linker between coumarin and 1,3,4-oxadizole is important for the inhibitory effect against AChE. Also, there is remarkable decrease in the activity of the compounds having the linkers (vinyl) between the 1,3,4-oxadiazole ring and the di or trihydroxy containing phenyl ring. It was also noticed that there is considerable decrease in activity if any of the hydroxyl group of the phenol is replaced by other electron donating methoxy or methylenedioxy groups. The docking studies results showed these potent compounds act through the inhibition of both AChE and BuChE. Further investigations and modification of these proposed compounds can lead to the development of highly potent therapeutics for the treatment of AD.

Declaration of Competing Interest

The authors declare that they have no known competing financial interests or personal relationships that could have appeared to influence the work reported in this paper.

Acknowledgement

Appendix A. Supplementary data

Supplementary data to this article can be found online at https://doi.org/10.1016/j.jksus.2022.101977.

References

Annunziata, F., Pinna, C., Dallavalle, S., Tamborini, L., Pinto, A., 2020. An Overview of Coumarin as a Versatile and Readily Accessible Scaffold with Broad-Ranging Biological Activities. Int. J. Mol. Sci. 21 (13), 4618.

Athar, T., Al Balushi, K., Khan, S.A., 2021. Recent advances on drug development and emerging therapeutic agents for Alzheimer's disease. Mol. Biol. Rep. 48 (7), 5629–5645.

Azmi, S.N.H., Al-Balushi, M., Al-Siyabi, F., Al-Hinai, N., Khurshid, S., 2020. Adsorptive removal of Pb (II) ions from groundwater samples in Oman using carbonized *Phoenix dactylifera* seed (Date stone). J. King Saud Univ.-Sci. 32 (7), 2931–2938.

Azmi, S.N.H., Al-Jassasi, B.M.H., Al-Sawafi, H.M.S., Al-Shukaili, S.H.G., Rahman, N., Nasir, M., 2021. Optimization for synthesis of silver nanoparticles through response surface methodology using leaf extract of Boswellia sacra and its application in antimicrobial activity. Environ. Monit. Assess. 193 (8).

Azmi, S.N.H., Al-Masrouri, Z.N., Al-Lamki, I.R., et al., 2022. Development and validation of spectrophotometric method for determination of imipramine hydrochloride concentration in solid materials: Case study. J. King Saud Univ. Sci. 101823.

Benek, O., Korabecny, J., Soukup, O., 2020. A perspective on multi-target drugs for Alzheimer's disease. Trends Pharmacol. Sci. 41 (7), 434–445.

Blume, T., Filser, S., Jaworska, A., Blain, J.-F., Koenig, G., Moschke, K., Lichtenthaler, S. F., Herms, J., 2018. BACE1 Inhibitor MK-8931 Alters Formation but Not Stability of Dendritic Spines. Front. Aging Neurosci. 10. https://doi.org/10.3389/fnagi.2018.00229.

Breijyeh, Z., Karaman, R., 2020. Comprehensive Review on Alzheimer's Disease: Causes and Treatment. Molecules 25 (24). https://doi.org/10.3390/molecules25245789.

Brookmeyer, R., Johnson, E., Ziegler-Graham, K., Arrighi, H.M., 2007. Forecasting the global burden of Alzheimer's disease. Alzheimers Dement. 3 (3), 186–191.

Cavalli, A., Bolognesi, M.L., Minarini, A., Rosini, M., Tumiatti, V., Recanatini, M., Melchiorre, C., 2008. Multi-target-directed ligands to combat neurodegenerative diseases. J. Med. Chem. 51 (3), 347–372.

Chaves, S., Várnagy, K., Santos, M.A., 2021. Recent Multi-target Approaches on the Development of Anti- Alzheimer's Agents Integrating Metal Chelation Activity. Curr. Med. Chem. 28 (35), 7247–7277. https://doi.org/10.2174/0929867328666210218103220.

Cheignon, C., Tomas, M., Bonnefont-Rousselot, D., Faller, P., Hureau, C., Collin, F., 2018. Oxidative stress and the amyloid beta peptide in Alzheimer's disease. Redox Biol. 14, 450–464.

Dey, I., Keller, K., Belley, A., Chadee, K., 2003. Identification and characterization of a cyclooxygenase-like enzyme from Entamoeba histolytica. Proc. Natl. Acad. Sci. 100 (23), 13561–13566.

Francis, P.T., Palmer, A.M., Snape, M., Wilcock, G.K., 1999. The cholinergic hypothesis of Alzheimer's disease: a review of progress. J. Neurol. Neurosurg. Psychiatry 66 (2), 137–147.

Guillozet-Bongaarts, A.L., Garcia-Sierra, F., Reynolds, M.R., Horowitz, P.M., Fu, Y., Wang, T., Cahill, M.E., Bigio, E.H., Berry, R.W., Binder, L.I., 2005. Tau truncation during neurofibrillary tangle evolution in Alzheimer's disease. Neurobiol. Aging 26 (7), 1015–1022.

Gupta, S., Nair, A., Jhawat, V., Mustaq, N., Sharma, A., Dhanawat, M., Khan, S.A., 2020. Unwinding complexities of diabetic Alzheimer by potent novel molecules. Am. J. Alzheimer's Dis. Other Dementias®, 351533317520937542.

Hamulakova, S., Poprac, P., Jomova, K., Brezova, V., Lauro, P., Drostinova, L., Jun, D., Sepsova, V., Hrabinova, M., Soukup, O., Kristian, P., Gazova, Z., Bednarikova, Z., Kuca, K., Valko, M., 2016. Targeting copper(II)-induced oxidative stress and the acetylcholinesterase system in Alzheimer's disease using multifunctional tacrine-coumarin hybrid molecules. J. Inorg. Biochem. 161, 52–62.

Husain, A., Balushi K, A.l., Akhtar, M.J., Khan, S.A., 2021. Coumarin linked heterocyclic hybrids: A promising approach to develop multi target drugs for Alzheimer's disease. J. Mol. Struct. 1241, 130618.

Karade, N.N., Gampawar, S.V., Shinde, S.V., Jadhav, W.N., 2007. L-proline catalyzed solvent-free knoevenagel condensation for the synthesis of 3-substituted coumarins. Chin. J. Chem . 25 (11), 1686–1689.

Khan, M.S.Y., Akhtar, M., 2003. Synthesis of some new 2,5-disubstituted 1,3,4-oxadiazole derivatives and their biological activity. Ind. J. Chem. 42B (4), 900–904.

Khokar, R., Hachani, K., Hasan, M., et al., 2021. Anti-Alzheimer potential of a waste by-product (peel) of Omani pomegranate fruits: Quantification of phenolic compounds, in-vitro antioxidant, anti-cholinesterase and in-silico studies. Biocatal. Agric. Biotechnol. 38, 102223.

Kumar, A., Singh, A., 2015. A review on Alzheimer's disease pathophysiology and its management: an update. Pharmacol. Rep. 67 (2), 195–203.

Lee, S.-Y., Chiu, Y.-J., Yang, S.-M., Chen, C.-M., Huang, C.-C., Lee-Chen, G.-J., Lin, W., Chang, K.-H., 2018. Novel synthetic chalcone-coumarin hybrid for Aβ aggregation reduction, antioxidation, and neuroprotection. CNS Neurosci. Ther. 24 (12), 1286–1298.

Liu, P.-P., Xie, Y., Meng, X.-Y., et al., 2019. History and progress of hypotheses and clinical trials for Alzheimer's disease. Signal Transduction and Targeted Therapy. 4 (1), 1–22.

Liu, Z., Li, T., Li, P., et al., 2015. The ambiguous relationship of oxidative stress, Tau hyperphosphorylation, and autophagy dysfunction in Alzheimer's disease. Oxid Med Cell Longev. https://doi.org/10.1155/2015/352723.

Lolak, N., Boga, M., Tuneg, M., Karakoc, G., Akocak, S., Supuran, C.T., 2020. Sulphonamides incorporating 1,3,5-triazine structural motifs show antioxidant, acetylcholinesterase, butyrylcholinesterase, and tyrosinase inhibitory profile. J. Enzyme Inhib. Med. Chem. 35 (1), 424–431.

Lovell, M.A., Xiong, S., Xie, C., Davies, P., Markesbery, W.R., 2005. Induction of hyperphosphorylated tau in primary rat cortical neuron cultures mediated by oxidative stress and glycogen synthase kinase-3. J. Alzheimers Dis. 6 (6), 659–671.

Macklin, L.J., Schwans, J.P., 2020. Synthesis, biochemical evaluation, and molecular modeling of organophosphate-coumarin hybrids as potent and selective butyrylcholinesterase inhibitors. Bioorg. Med. Chem. Lett. 30, (13). https://doi.org/10.1016/j.bmcl.2020.127213 127213.

Makhaeva, G.F., Kovaleva, N.V., Rudakova, E.V., Boltneva, N.P., Lushchekina, S.V., Faingold, I.I., Poletaeva, D.A., Soldatova, Y.V., Kotelnikova, R.A., Serkov, I.V., Ustinov, A.K., Proshin, A.N., Radchenko, E.V., Palyulin, V.A., Richardson, R.J., 2020. New Multifunctional Agents Based on Conjugates of 4-Amino-2,3-polymethylenequinoline and Butylated Hydroxytoluene for Alzheimer's Disease Treatment. Molecules 25 (24), 5891.

Martyn, C., 2003. Anti-inflammatory drugs and Alzheimer's disease. BMJ 327 (7411), 353–354. https://doi.org/10.1136/bmj.327.7411.353.

Molyneux, P., 2004. The use of the stable free radical diphenylpicrylhydrazyl (DPPH) for estimating antioxidant activity. Songklanakarin J. Sci. Technol. 26 (2), 211–219.

Moya-Alvarado, G., Yañez, O., Morales, N., González-González, A., Areche, C., Núñez, M.T., Fierro, A., García-Beltrán, O., 2021. Coumarin-chalcone hybrids as inhibitors of MAO-B: biological activity and *in Silico* studies. Molecules 26 (9), 2430.

Nazari, M., Rezaee, E., Hariri, R., et al., 2021. Novel 1,2,4-oxadiazole derivatives as selective butyrylcholinesterase inhibitors: Design, synthesis and biological evaluation. Excli J. 20, 907–921. https://doi.org/10.17179/excli2021-3569.

Shaik, J.B., Palaka, B.K., Penumala, M., Kotapati, K.V., Devineni, S.R., Eadlapalli, S., Darla, M.M., Ampasala, D.R., Vadde, R., Amooru, G.D., 2016. Synthesis, pharmacological assessment, molecular modeling and in silico studies of fused tricyclic coumarin derivatives as a new family of multifunctional anti-Alzheimer agents. Eur. J. Med. Chem. 107, 219–232.

Simone Tranches Dias, K., Viegas, C., 2014. Multi-target directed drugs: a modern approach for design of new drugs for the treatment of Alzheimer's disease. Curr. Neuropharmacol. 12 (3), 239–255.

Small, D.H., Cappai, R., 2006. Alois Alzheimer and Alzheimer's disease: A centennial perspective. J. Neurochem. 99 (3), 708–710.

Stefanachi, A., Leonetti, F., Pisani, L., Catto, M., Carotti, A., 2018. Coumarin: A natural, privileged and versatile scaffold for bioactive compounds. Molecules 23 (2), 250.

Szwajgier, D., Borowiec, K., Pustelniak, K., 2017. The neuroprotective effects of phenolic acids: molecular mechanism of action. Nutrients. 9 (5), 477. https://doi.org/10.3390/nu9050477.

WHO, 2012. Dementia: a public health priority, World Health Organization.

Wimo, A., Jönsson, L., Bond, J., Prince, M., Winblad, B., 2013. The worldwide economic impact of dementia 2010. Alzheimers Dement. 9 (1), 1–11.e13.

Zhang, J., Li, J.-C., Song, J.-L., Cheng, Z.-Q., Sun, J.-Z., Jiang, C.-S., 2019. Synthesis and evaluation of coumarin/1,2,4-oxadiazole hybrids as selective BChE inhibitors with neuroprotective activity. J. Asian Nat. Prod. Res. 21 (11), 1090–1103.